International Journal of Nanomedicine

Dovepress
open access to scientific and medical research

Open Access Full Text Article

ORIGINAL RESEARCH

In silico Prediction of *Malvaviscus arboreus* Metabolites and Green Synthesis of Silver Nanoparticles – Opportunities for Safer Anti-Bacterial and Anti-Cancer Precision Medicine

Afrah E Mohammed[1,*], Sahar S Alghamdi[2,3], Ashwag Shami[1,*], Rasha Saad Suliman[4], Kawther Aabed[1], Modhi O Alotaibi[1], Ishrat Rahman[5]

[1]Department of Biology, College of Science, Princess Nourah bint Abdulrahman University, Riyadh, 11671, Saudi Arabia; [2]Department of Pharmaceutical Sciences, College of Pharmacy, King Saud Bin Abdulaziz University for Health Sciences, Riyadh, Saudi Arabia; [3]King Abdullah International Medical Research Center (KAIMRC), Riyadh, Saudi Arabia; [4]Department of Pharmacy, Fatima College of Health Sciences, Abu Dhabi, 3798, United Arab Emirates; [5]Department of Basic Dental Sciences, College of Dentistry, Princess Nourah bint Abdulrahman University, Riyadh, 11671, Saudi Arabia

*These authors contributed equally to this work

Correspondence: Ishrat Rahman, Department of Basic Dental Sciences, College of Dentistry, Princess Nourah bint Abdulrahman University, P.O. Box 84428, Riyadh, 11671, Saudi Arabia, Email imrahman@pnu.edu.sa

Introduction: Biogenic silver nanoparticles (AgNPs) may be a feasible therapeutic option in the research and development towards selectively targeting specific cancers and microbial infections, lending a role in precision medicine. In-silico methods are a viable strategy to aid in drug discovery by identifying lead plant bioactive molecules for further wet lab and animal experiments.

Methods: Green synthesis of M-AgNPs was performed using the aqueous extract from the *Malvaviscus arboreus* leaves, characterized using UV spectroscopy, FTIR, TEM, DLS, and EDS. In addition, Ampicillin conjugated M-AgNPs were also synthesized. The cytotoxic potential of the M-AgNPs was evaluated using the MTT assay on MDA-MB 231, MCF10A, and HCT116 cancer cell lines. The antimicrobial effects were determined using the agar well diffusion assay on methicillin-resistant *S. aureus* (MRSA) and *S. mutans, E. coli*, and *Klebsiella pneumoniae*. Additionally, LC-MS was used to identify the phytometabolites, and in silico techniques were applied to determine the pharmacodynamic and pharmacokinetic profiles of the identified metabolites.

Results: Spherical M-AgNPs were successfully biosynthesized with a mean diameter of 21.8 nm and were active on all tested bacteria. Conjugation with ampicillin increased the susceptibility of the bacteria. These antibacterial effects were most predominant in *Staphylococcus aureus* ($p < 0.0001$). M-AgNPs had potent cytotoxic activity against the colon cancer cell line (IC_{50}=29.5 µg/mL). In addition, four secondary metabolites were identified, Astragalin, 4-hydroxyphenyl acetic acid, Caffeic acid, and Vernolic acid. In silico studies identified Astragalin as the most active antibacterial and anti-cancer metabolite, binding strongly to the carbonic anhydrase IX enzyme with a comparatively higher number of residual interactions.

Discussion: Synthesis of green AgNPs presents a new opportunity in the field of precision medicine, the concept centered on the biochemical properties and biological effects of the functional groups present in the plant metabolites used for reduction and capping. M-AgNPs may be useful in treating colon carcinoma and MRSA infections. Astragalin appears to be the optimal and safe lead for further anti-cancer and anti-microbial drug development.

Keywords: biogenic AgNPs, LC-MS, Astragalin, biological activity

Introduction

Nanoparticles are submicroscopic uniform particulate structures ranging from 1nm to 100nm in diameter. They feature a high surface area-to-size ratio and provide immense properties and applications in the food, cosmetic, agriculture, chemical, engineering, imaging, pharmaceutical, and medical industries. They can be classified in various ways based on

Received: 27 December 2022
Accepted: 20 March 2023
Published: 26 April 2023

their shape, material properties, application, synthesis, and chemical origin, either organic or inorganic. Liposomes and dendrimers are organic, whereas metal nanoparticles such as silver and gold, and fullerenes are inorganic.[1]

Ease in design and manipulation of nanoparticles have led to the formation of nano-vaccines and nano-therapy, benefiting the pharmaceutical and medical industry. Their advantages are far-fetched, providing efficient absorption of drugs and complete distribution into tissues, as well as acting as an efficient, targeted transport vehicle, providing imaging and safer alternatives to treating cancers and other diseases, where traditional therapy can be a failure due to toxic side effects.

Silver nanoparticles (AgNPs) are well studied and known to be a stable type of nanoparticle. Their use, applications, and toxicities are understood and have been evaluated.[2–4] Typically, AgNPs can be synthesized using a variety of methods, such as physical methods: laser irradiation, electrical irradiation, gamma irradiation, evaporation-condensation, and microemulsion techniques.[5] They can also be chemically synthesized by chemical reduction using organic or inorganic reducing agents, which reduce Ag^{+} forming Ag^{0}, resulting in clustering and agglomeration. Surfactants and capping agents can be used to prevent growth and large aggregates from forming, stabilizing the nanoparticulate structure, and maintaining its surface properties. An additional component in the chemical synthesis that affects the size, shape, stability, and properties of the formed nanoparticles is heat and light, for instance, using photo-reduction or UV-reduction.[5]

The benefits of green synthesized NPs are remarkable, as well as yielding stable, uniform, and compact NPs, and the synthesis can be convenient, cost-effective, and safe, in addition to giving enhanced therapeutic value depending on the intrinsic properties and utilization of the plant, bacteria, fungi, or algae used in the reduction process. Important to note is that plants may be the preferred green source over microorganisms due to the requirement to culture microorganisms in their appropriate environment, in addition to issues related to pathogenicity and disease. Therefore, plants are a simpler, cost-effective, and eco-friendly source of green NPs.[6] The entire plant/medicinal herb or different parts: roots, stem, leaves, and flowers can be used to prepare either aqueous, ethanolic, methanolic extracts or extracts in various solvents for the synthesis of green NPs. These extracts contain a rich content of phytochemicals and useful secondary metabolites such as proteins, enzymes, amino acids, fatty acids, vitamins, oligosaccharides, alkaloids, flavonoids, glycosides, phenolics, saponins, steroids, quinones, sequesterones, terpenes, and tannins having great therapeutic value and potential as future drugs with activities such as antioxidant, anti-inflammatory, analgesic, wound healing, immunomodulatory, cytotoxic, anti-coagulant, and anti-microbial to name a few.[7–10]

Cancer cases are increasing worldwide, and selective therapeutic treatment options are limited. Research and development on novel treatment strategies are a priority, as is the identification of newer antibiotics to tackle resistance and failed antibiotic treatment options due to rampant overuse and poor prescribing. Many therapeutic cancer drugs, such as anti-metabolites, arrest the cell cycle and can resemble the structure of purines and pyrimidines.[11] Another option to consider is to use AgNPs to either cause apoptosis or necrosis, and biogenic synthesis of AgNPs may be a selective and cost-effective option. In this study, we focused our efforts on assessing the potential of *Malvaviscus arboreus* (rarely studied plant) as a source of bioactive phytochemicals in the field of drug discovery to produce targeted and effective treatments for cancer and microbial infections by using *M. arboreus* green synthesized NPs.

Malvaviscus arboreus is from the Hibiscus family native to America, Latin, Central, and the South.[12] It is also commonly known as Sleeping Hibiscus or Wax Mallow and is used in salads, teas, and dyes.[13] *M. arboreus* has a strong medicinal value. In parts of India, the plant has been used for hair growth. One study tested various fractions of the plant extract, ethanolic, n-hexane, ethyl acetate, and aqueous against the positive control 15% minoxidil, yielding comparable results.[14] Furthermore, the petroleum ether fraction, dichloromethane, ethyl acetate, and aqueous fractions from the aerial part of *M. arboreus* had hepatoprotective effects.[15] Rats were given the fractions orally for 6 days, followed by induction of hepatotoxicity by carbon tetrachloride. Pre-dosage with the fractions prevented toxic effects, indicated by reduced ALT, AST, ALP, bilirubin, and malondialdehyde, as compared to the positive control (rats with carbon-tetrachloride induced hepatotoxicity with no prior oral consumption of plant extract). In addition, the plant fractions improved hepatic antioxidant capacity.[15] The use of *M. arboreus* to help in stomach ailments suggests gastroprotective effects for the herb, and one study identified that two glycosylated flavonoids richly found in the ethyl acetate fraction were notably responsible for gastroprotective effects seen in a rat model of ethanol-induced gastric ulcer.[16] In addition, *M. arboreus*

aqueous leaf extract had antimicrobial effects on human pathogenic bacteria *Pseudomonas aeruginosa, Escherichia coli* 25922, and *Listeria monocytogenes*,[17] and the dichloromethane fraction of *M. arboreus* was active against protozoal infections having anti-Trypanosoma effects and had anti-protease activity.[18] An earlier study identified the crude methanolic extract of *M. arboreus* to have potent antioxidant activity and moderate erythrocyte membrane stabilizing effect, as demonstrated in an assay assessing the heat and hypnotic-induced hemolysis of RBCs.[19] Thus, the therapeutic potential of this herb seems wide and varied. However, the literature available on the anti-cancer effects of *M. arboreus* and its metabolites is scarce.

Our objectives were to produce AgNPs using *M. arboreus* plant extract, identify their biological cytotoxic application on breast cancer cells and colon cancer cells, and test the microbial activity against a panel of bacteria. In addition, we wanted to identify the active phytochemicals from the aqueous extract of the herb and use in silico techniques to predict the bioactivity, pharmacodynamics, and pharmacokinetics to find a potential lead for further research and development.

Materials and Methods

The Collection and Preparation of Plant Material

Malvaviscus arboreus leaves were collected from the local nursery, Royal Commission for Riyadh City Nursery, Saudi Arabia. Plants were identified based on confirmed characteristics and were stored at 4 °C in polythene bags until used. The leaves were washed and dried, after which a fine powder was prepared by a milling machine (IKA-Werke, GMBH and Co., Germany). Finally, the milled material was kept in sterile plastic bags at room temperature for further use.

Plant Extraction and AgNPs Fabrication

An aqueous extract from the leaf powder was produced by adding a ratio of 2:100 distilled water (w/v). The solution was heated for 10 min at 80 °C and subsequently filtered using Whatman grade No. 1 filter paper (125 mm diameter and 11 µm mean pore size). The resulting supernatant was used for AgNP synthesis. Briefly, in a flask, 90 mL of $AgNO_3$ (1mM) was added to the plant extract (10 mL) in and heated at 80°C for 15 min. The reaction was allowed to continue at room temperature for 24 h in the dark until a sable brown color was observed. The mixture was then centrifuged for 15 min at 14,000 rpm, the supernatant was aspirated, and the pellet was washed in distilled water and then allowed to dry at room temperature. Further experiments were performed using 1 mg/mL M-AgNPs prepared in distilled water.

Characterization of Bio-Fabricated AgNPs

In the present investigation, several techniques, as listed below, were performed for the characterization of the biogenic AgNPs (M-AgNPs).

Ultraviolet-Visible Spectroscopy

Color variation was visually observed when $AgNO_3$ was incubated with the *Malvaviscus arboreus* leaves extract. After the 24 h incubation, the UV–Visible absorption spectra were measured using a spectrophotometer (UV–Vis) (BIOCHROM Libra S60PC, Serial Number: 119377, England) at 300–600 nm.[20]

Electronic Transmission Microscope (TEM)

The M-AgNPs morphology and size distribution were examined by TEM (JEM-1011, JEOL, Japan) at 80 kV and scanning electron microscopy (SEM) (JEOL, JED-2200 series, Japan). A drop of NPs solution was added to a carbon-coated copper grid (200 mesh). Then, the grid was dried using a vacuum desiccator.[21]

Dynamic Light Scatter (DLS)

The pattern of M-AgNPs size distribution has been detected using dynamic light scattering, and zeta potential was evaluated using Zetasizer advanced series (Malvern Panalytical Ltd, WR141XZ, United Kingdom).[22]

Elemental Analysis

Scanning electronic microscope with energy-dispersive X-ray spectroscopy (EDS) was attained to determine the surface analysis of the M-AgNPs and the incorporation of the silver element.[23]

Functional Group Detection

Fourier-transform infrared spectroscopy (FTIR) analysis using SPECTRUM100, Perkin-Elmer, USA, was conducted to identify the probable *Malvaviscus arboreus* secondary metabolites involved in the reduction process of the extract and $AgNO_3$. Data were established at a range of 450–3500 cm^{-1}.

Biological Activity of AgNPs

Antibacterial Screening

Agar well diffusion and antibacterial susceptibility test (AST) were conducted to identify the antibacterial efficacy of the treatments on four pathogenic bacteria: *E. coli*, *Klebsiella pneumoniae* (gram-negative), methicillin-resistant *S. aureus* (MRSA) and *S. mutans* (gram-positive). Subcultures were grown from each strain on Nutrient agar medium (Oxoid) for 24 h at 37°C. Bacterial suspensions of 1.5×10^8 CFU/mL (McFarland standard, 0.5) were prepared. Under sterile conditions, agar plates were inoculated with 1 of each type of bacterial strain, and 40 microliters of plant extract and M-AgNPs (1mg/mL) were added independently to a well and dried. Distilled water and ampicillin were applied as negative and positive controls, respectively. Thereafter, plates have been kept at 37 °C for 24h, and the inhibition zone for each loaded well was detected in mm.[24]

Synthesis and Application of Ampicillin-Conjugated M-AgNPs

A method used by Fan et al[25] was adopted and modified to synthesize nanocomposite (Amp-M-AgNPs). Briefly, equal volumes of ampicillin (1mg/mL) and M-AgNPs (1mg/mL) were mixed at room temperature for 48 h in the dark.[25] The standard agar well diffusion method was used to assess the antimicrobial activity, as described above (Antibacterial Screening).

Assessment of Cell Viability

The cell viability was assessed by MTT assay as explained previously[9] to determine the cytotoxic effects of M-AgNPs on HCT116 (colorectal carcinoma cell line), MDA MBA 231 (breast cancer), and a breast epithelial cell line used as a control (MCF 10A). All cell lines were commercial from ATCC, USA, MDA MB-231 (HTB-26); HCT116 (CCL-247) and MCF 10A (RL-10317). Experiments were conducted in 96 well plates, and cells were seeded (5×10^4 cells/well) and grown at 37 °C in 95%/5% humidified air/CO_2 condition atmosphere. Cells have then been subjected to different doses of M-AgNPs at concentrations ranged between 2.05–4200 μg/mL and incubated for 48 h.

LC-QTOF-MS Analysis

An aqueous extract of the plant was produced by mixing leaf powder with distilled water and placing it on heat at 60 ◦C for 48 h before filtration with Grade 1 Whatman paper and finally evaporation. The dry plant extract (1mg) was added to methanol (1 mL) and analyzed by LC-QTOF-MS as described previously. The MS data was generated using the Agilent Mass Hunter qualitative and quantitative analysis software (Agilent Technologies). Thereafter, the Molecular Feature Extraction (MFE) algorithm and recursive analysis workflow were used to identify the chemical features from the LC-MS data.

Silico Pharmacological Properties

Prediction of Anticancer Activity of *Malvaviscus arboreus* Metabolites

The bioactive metabolites of *Malvaviscus arboreus* were identified using LC-MS, and the Chemdraw tool was used to draw the 2D chemical structures of the identified metabolites. The SMILES (Simplified Molecular Input Line Entry System) for each identified molecule was generated and used in the PASS online webserver to predict the activity.[26] The web server gives a probability for a compound to be active or inactive on a specific biological response based on a training set that contains biologically active molecules (http://way2drug.com/passonline/faq.php).

Predictions of Molecular Targets

Three web servers were operated to predict potential biological targets for *Malvaviscus arboreus* secondary metabolites, including SWISS Target predictions (http://www.swisstargetprediction.ch/), Sea Search (https://sea.bkslab.org/), and Molinspiration (https://www.molinspiration.com/). These online tools predict the molecular targets of small molecules

using a similarity approach for a known active library.[27,28] For each molecule, the 2D structures from SMILES were used as the input for each tool to generate the predictions.

Molecular Docking of Identified Metabolites into the Crystal Structure of Human Carbonic Anhydrase (CA) IX Enzyme

A docking study on the Carbonic Anhydrase IX crystal structure (PDB: 5FL6) was performed for each identified secondary metabolite. The LigPrep tool (LigPrep, Schrödinger) was used to prepare the 2D chemical structures for the secondary active metabolites. Also, the protein grid was generated via a receptor grid generation tool available in Maestro software (Receptor Grid Generation Panel, Schrödinger).[29] The docking study and the poses generated were qualitatively and quantitatively analyzed using Glide (Glide, Schrödinger).

Molecular Dynamics Simulation of Protein-Ligand Complex

The metabolite that demonstrated the best docking score and interaction was further analyzed using Desmond (Desmond, Schrödinger), in which a molecular simulation was performed. The parameters used for generating the simulation complex were TIP4P water molecules (8411), neutralization of the system by adding 6 Na^+, and NPT ensemble were applied for conducting the simulation run. The simulation was conducted for a time scale of 100 ns, and the complex was relaxed before starting the production run. A simulation interaction diagram (SID) was used for post-simulation analysis.

Absorption, Distribution, Metabolism, and Excretion (ADME) Properties Predictions for *Malvaviscus arboreus* Secondary Metabolites

The QikProp (QikProp, Schrödinger LLC New York, NY) and SWISS ADME (http://www.swissadme.ch/)[30] computational tools were employed to predict the important physicochemical properties for the bioactive molecules identified in *Malvaviscus arboreus* extract. The predicted physicochemical properties include Molecular Weight, lipophilicity (Log Po/w), solubility (Log S), blood–brain barrier penetration (BBB Permeant), oral gastrointestinal absorption (GI Absorption), and violations of Lipinski's rule of five (ROF).

The Profile of Cytochromes (CYP) P450 Enzymes Inhibition for *Malvaviscus arboreus* Metabolites

SWISS ADME webserver was utilized to see the effect of the secondary metabolites identified in *M. arboreus* extract on five important cytochrome P-450 enzymes, including CYP1A2, CYP2C19, CYP2C9, CYP2D6, and CYP3A4 (http://www.swissadme.ch/index.php). The web server predicts whether a small molecule is an inhibitor for CYP enzymes or not.

Organ Toxicity and Safety Predictions for *Malvaviscus arboreus* Metabolites

ProTox-II webserver was utilized to predict the potential toxicity of the secondary metabolites identified in *Malvaviscus arboreus* Extract using SMILES as an input to generate the predictions. Several types of toxicity were evaluated including hepatotoxicity, carcinogenicity, cytotoxicity, mutagenicity, and immunotoxicity for the four metabolites.[31]

Statistical Analysis of the Data

Means and standard deviations were calculated for the antibacterial activities using MICROSOFT EXCEL 2019. For all images, a representation from among three individual experiments is shown. Data were statistically analyzed using GraphPad Prism Software version 9.1 (San Diego, California, USA). The ImageJ software (National Institutes of Health, Bethesda, MD, United States) was utilized to calculate the size of the NPs.

Results

Biogenic Silver Nanoparticles (AgNPs)

This study aimed to examine the benefits of using *M. arboreus* aqueous leaf extract as bio-mediators in the fabrication of AgNPs and determine the anticancer and antibacterial activities of the aqueous leaf extract and the resulting M-AgNPs. The plant extract was added to a solution of $AgNO_3$, which produced a mixture that altered color from pale yellow to brown-yellow. M-AgNPs biosynthesis progression underwent a transition, first a slow color alteration in the reaction medium over a period of 20 h incubation time, then the strength of the color increased during the residual reaction time.

M-AgNPs Properties

Physicochemical Characterization of AgNPs

The formation of the nanoparticles in the aqueous solution of *M. arboreus* leaves was additionally confirmed by UV–visible spectroscopy. The solution was scanned on a fixed wavelength scale between 300 and 500 nm, and characteristic of silver nanoparticles, a maximum absorbance was observed at 436.59 nm (Figure 1).

The M-AgNPs were further categorized using TEM and DLS. The TEM image showed that the M-AgNPs were well dispersed, and their shapes were mostly spherical as clear from Figure 2 where images were taken at varied magnifications and the mean diameter of the M-AgNPs was 21.8 ± 1.1 nm. Further, M-AgNPs showed mean sizes of 115.6 ± 2.3 nm, as measured via DLS technique with PDI 0.204 (Figure 3A) and negative zeta potential (−31.59 ±0.7 mV) (Figure 3B).

The elemental composition and surface morphology were detected by using SEM/EDS. Figure 4A shows the morphology of M-AgNPs assembly as aggregates of spherical shape. The elemental components and the abundance of the biofabricated M-AgNPs were assimilated from EDS, as revealed in Figure 4B. The EDS spectrum shows the purity

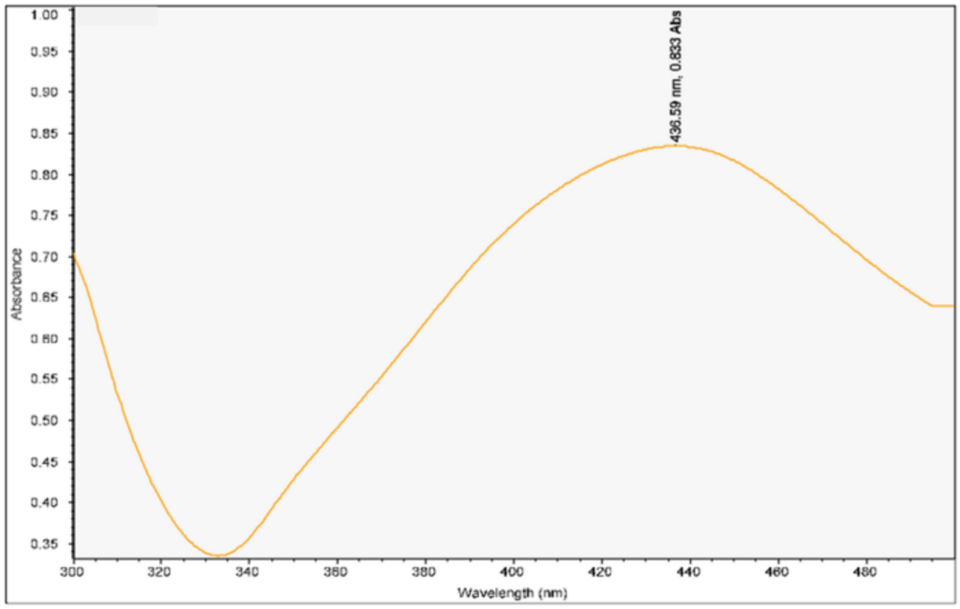

Figure 1 UV spectroscopy of M-AgNPs.

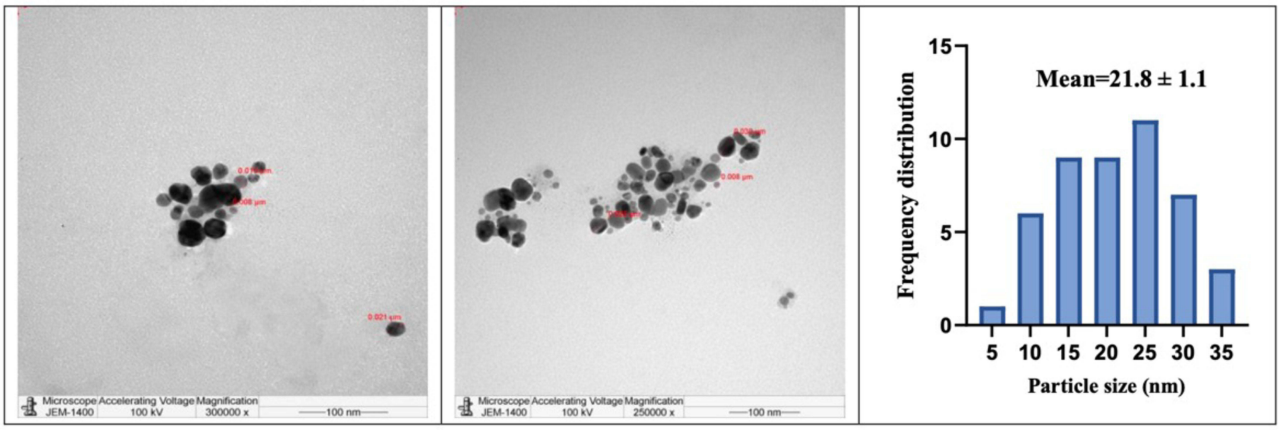

Figure 2 TEM analysis indicating the morphology and size of the M-AgNPs gained from *M. arboreus* aqueous extract at varied magnifications and their mean size diameter. Size measurements have been assessed from TEM micrographs at scale bars: 100 nm using ImageJ software constructed.

A

Sample Name:	3 3		
SOP Name:	mansettings.nano		
File Name:	Installation tests.dts	Dispersant Name:	Water
Record Number:	42	Dispersant RI:	1.330
Material RI:	1.59	Viscosity (cP):	0.8872
Material Absorbtion:	0.010	Measurement Date and Time:	Sunday, December 20, 2020 1:58:4...
Temperature (°C):	25.1	Duration Used (s):	60
Count Rate (kcps):	340.6	Measurement Position (mm):	4.65
Cell Description:	Disposable sizing cuvette	Attenuator:	8

			Size (d.nm):	% Intensity:	St Dev (d.nm):
Z-Average (d.nm):	115.6	Peak 1:	138.7	100.0	58.25
PdI:	0.204	Peak 2:	0.000	0.0	0.000
Intercept:	0.894	Peak 3:	0.000	0.0	0.000
Result quality :	Good				

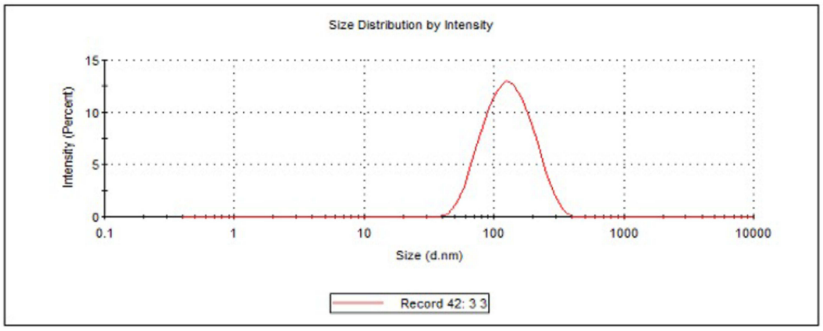

B

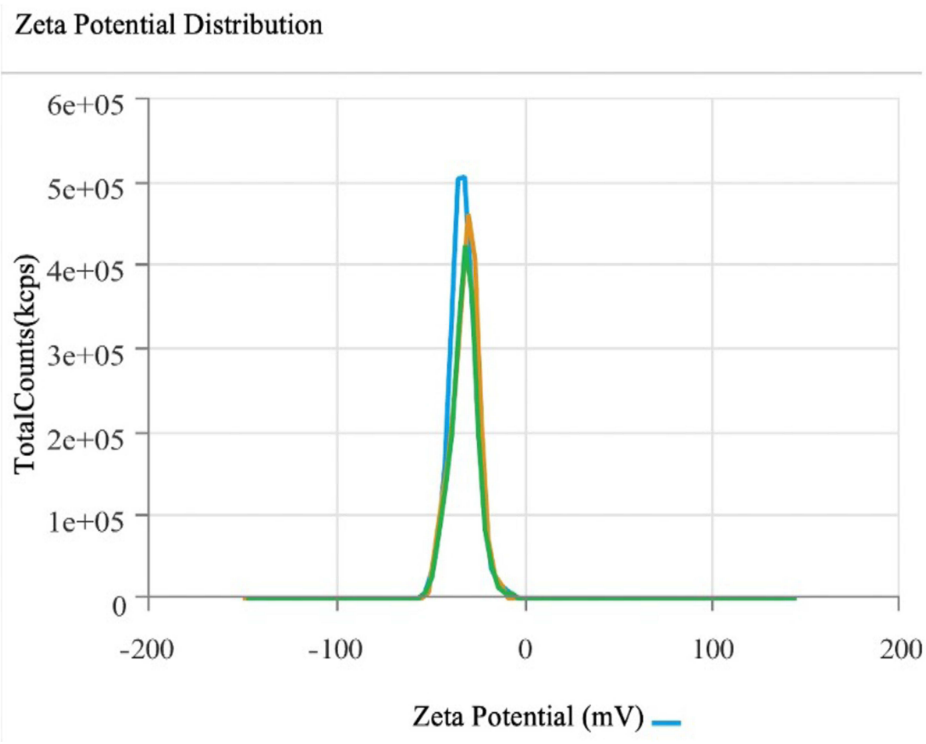

Figure 3 Size (**A**) and zeta potential distribution (**B**) of AgNPs obtained using the aqueous extracts of *M. arboreus*.

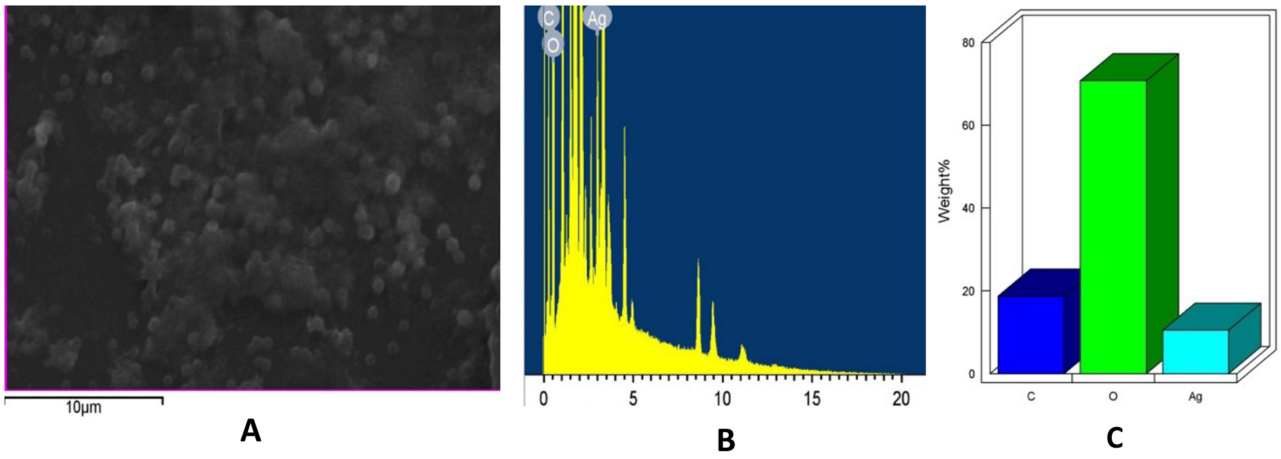

Figure 4 (**A**) SEM image (**B**) EDS spectrum (**C**) percentage relative composition of elements in M-AgNPs.

and the chemical conformation of M-AgNPs. The proportion of Ag construct in incidence with other chemical parts was considerable. The optical absorption characteristic peak at 3 keV was noted for the condensed M-AgNPs when analyzed by EDS. The EDS examination also displayed the percentage relative composition of elements such as Carbon (C) 18%, Oxygen (O) 70% and Silver (Ag) 10% (Figure 4C).

FTIR Evaluation

FTIR analysis has been taken to categorize the chemical transformation occurring through the interaction between the silver nitrate and functional clusters present in the *M. arboreus* extract. Comparing the FTIR data for M-AgNPs and the plant extract that exhibited in Figure 5 provides information about the diverse phytochemicals that could be involved in the reduction process of Ag ions into M-AgNPs. The peaks of absorption were identified at 3282.64, 2205.53, 2191.17, 2157.69, 2146.72, 2135.15, 2039.79, 2015.97, 1980.21, 1751.08 and 1635.69 cm^{-1} for *M. arboreus* extract (Figure 5A), while absorption peaks were detected with small alterations at 3262.28, 2204.23, 2181.92, 2167.28, 2140.42, 2122.15, 2039.77, 2019.33, 2003.85, 1994.34, 1973.07 and 1634.89 cm^{-1} for the M-AgNPs (Figure 5B).

Biological Activity of AgNPs

Antibacterial Effects of M-AgNPs and Antibiotic Nanocomposite

Antibacterial effect for the tested agents was identified for 0.4 mL/well against all investigated microbes as shown by the inhibition zone diameters in mm. The clear zone around the well contains tested agent at *S. mutans, K. pneumoniae, S. aureus*, and *E. coli* plates ranged between 7.5 ± 0.8 to 9.5 ± 0.5 mm when *M. arboreus* extract was tested and 12 ± 0.8 to 27 ± 2.6 mm for M-AgNPs. The antibiotic ampicillin indicated inhibition zone ranged between 16.5 ± 1 to 19.5 ± 0.5 which increased significantly when conjugated with M-AgNPs that indicated inhibition zone ranged 18 ± 1 to 33.7 ± 0 mm as shown in Figure 6. A significant variation in the effects of the tested agents was reported for all tested bacteria ($p < 0.0001$). In addition, a significant difference in the interactions between bacteria for any one of the tested agents was also noted ($p < 0.0001$). The most sensitive bacterial strain was *S. aureus* against both M-AgNPs and its ampicillin conjugated form.

Cytotoxicity

The cytotoxic response of M-AgNPs on MDA MB 231, HCT116 and MCF10A cells was assessed by conducting MTT assays, and the results are shown in Figure 7. A dose-dependent cytotoxic response was observed in all cell lines tested. The M-AgNPs were more efficacious and potent on the HCT116 cells than on MDA MB 231 and MCF10A cell lines. The cytotoxic potency (IC_{50}) of the M-AgNPs in HCT116, MDA MB 231, and MCF10A cells were 29.5, 354.7, and 69.1 μg/mL, respectively (Figure 7). An IC_{50} value of less than 100 μg/mL was considered active, and anything

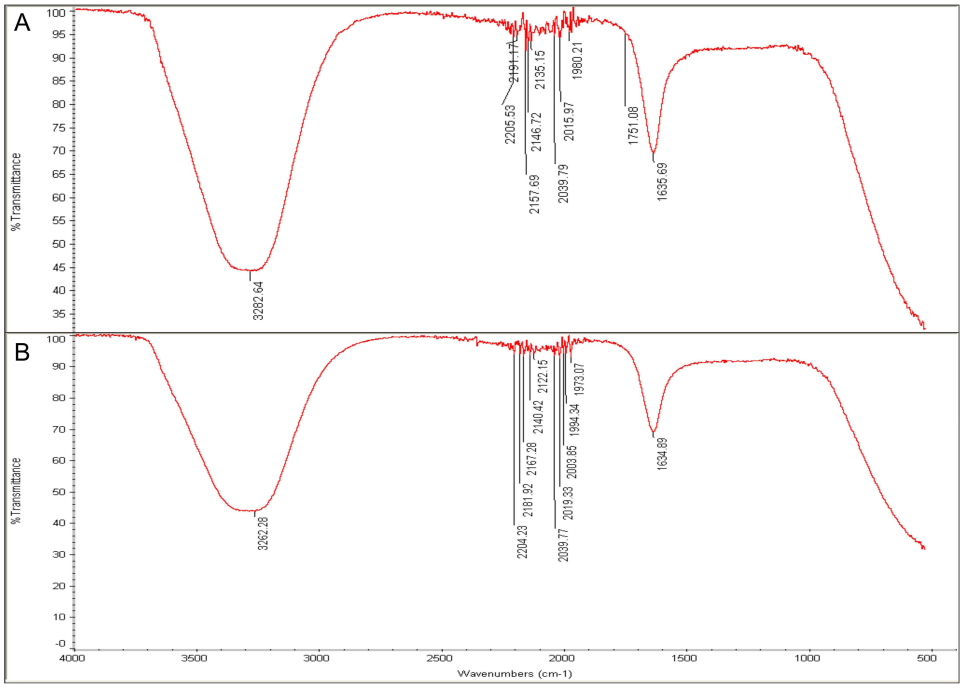

Figure 5 (**A**) FTIR analysis of *M. arboreus* extract and (**B**) M-AgNPs obtained using an aqueous extract of *M. arboreus*.

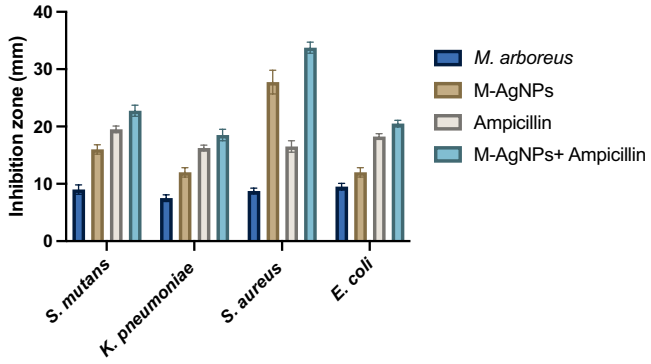

Figure 6 Antibacterial activities of *M. aroberus* extract, M-AgNPs, ampicillin and the ampicillin conjugated M-AgNPs. Data are expressed as the means ±SD (n=4).

above 100 µg/mL was considered inactive. As such, the M-AgNPs had the most potent cytotoxic effect on the HCT116 cells (IC_{50}= 29.5 µg/mL) and then on MCF10A cells and inactive on MDA MB 231 cells.

Identification of Bioactive *M. arboreus* Metabolites

M. arboreus aqueous extract (1 mg) was dissolved in methanol and exposed to total ion current spectra (TIC) to identify the plant metabolites, the analysis results are shown in Figure 8. Mass screening was done, and then the chemical features from the LC-MS data were summarized using the recursive analysis workflow and the Molecular Feature Extraction (MFE) algorithm. Detected nodes at various retention times per minute were the features that have been used for screening, with a minimum intensity of 6000 counts, and aligned with earlier identified composites considering adducts ($[M+H]^+$, $[M+2H]^+$, $[M+3H]^+$, and $[M-H]^-$). The tentatively identified compounds were Astragalin (A), and 4-hydroxyphenylacetic acid (B)[15] Caffeic acid (C), and Vernolic acid (D).[32] Mean m/z implies measured m/z.

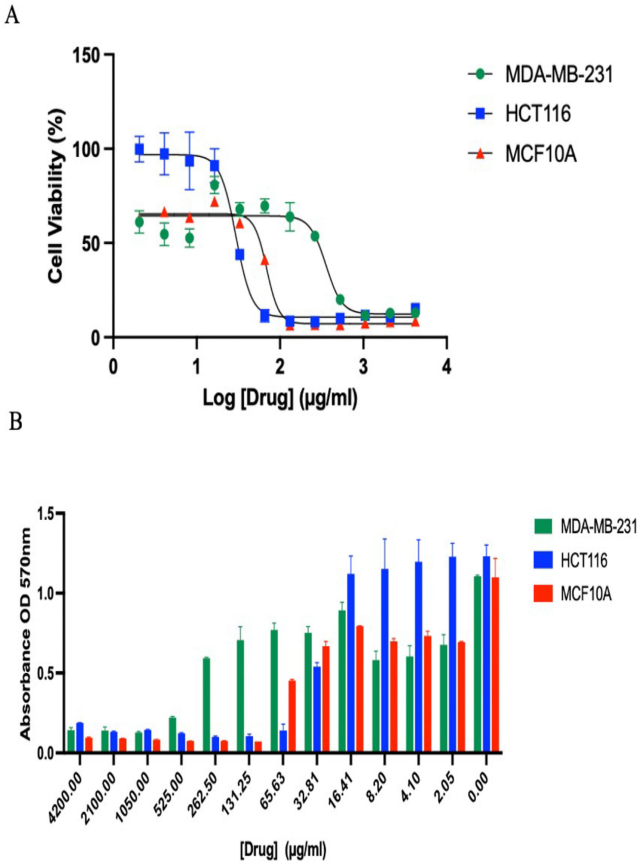

Figure 7 (**A**) Dose-response showing the cytotoxic effect of M-AgNPs on the cancer cell lines; MDA MB 231, HCT116, and MCF10A. (**B**) Summary of the anticancer ability of M-AgNPs on HCT116, MDA MB 231, and MCF10A cells treated for 24 hrs. M-AgNPs were examined at twelve varied concentrations ranging from 2.05 to 4200 µg/mL. The histograms columns display the mean ± SD (n = 4).

In silico Predictions of *M. arboreus* Secondary Metabolites Pharmacological Properties

Anti-Cancer Activity Predictions of *M. arboreus* Secondary Metabolites Using PASS

The anti-cancer biological activity of each secondary metabolite was predicted using the PASS online web server. Our results demonstrated that Astragalin possesses the highest anti-cancer activity, followed by Caffeic acid, Vernolic acid, and 4-hydroxyphenyl acetic acid, respectively (Table 1 and Figure 9). These results provide additional confirmation to the observed anti-cancer activity of *M. arboreus* against cancer cell lines.

Predictions of Molecular Targets for *M. arboreus* Secondary Metabolites Using SWISSADME, Sea Search, and Molinspiration

Using three different webservers, Astragalin, 4-hydroxyphenyl acetic acid, and Caffeic acid demonstrated similar prediction findings in which carbonic anhydrase enzyme could be the molecular target that mediated the observed anti-cancer and anti-bacterial responses (Table 2, and Figure 10). On contrary, Vernolic acid demonstrated a high probability score as an enzyme inhibitor; however, carbonic anhydrase was not predicted using SWISS target prediction and SEA search. Our present findings suggest that these bioactive metabolites could inhibit the carbonic anhydrase that produces beneficial anti-cancer and anti-bacterial activity.

Molecular Docking of *M. arboreus* Secondary Metabolites with Carbonic Anhydrase IX (CA IX) Crystal Structure Using Glide

In this study, we sought to investigate the protein–ligand interactions between the secondary metabolites identified in *M. arboreus* extract and the CA IX crystal structure. Thus, Glide was utilized to perform the molecular docking, and several poses were generated, as summarized in Table 3. Our docking results demonstrated that Astragalin possesses the

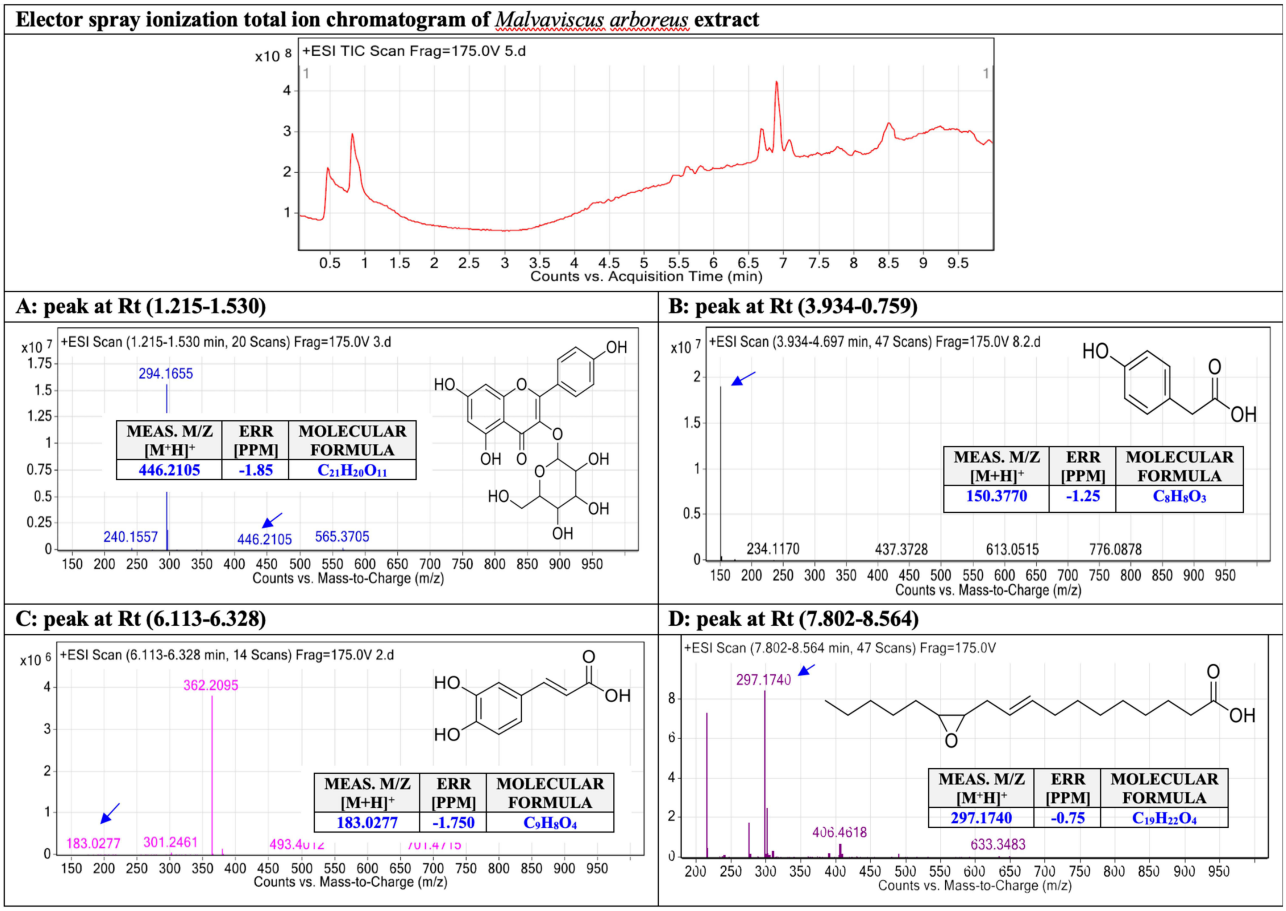

Figure 8 Base peak chromatogram of *M. arboreus* methanolic extract. The tentatively recognized biomolecules are Astragalin (**A**), and 4-hydroxyphenyl acetic acid (**B**), Caffeic acid (**C**), and Vernolic acid (**D**). Mean m/z implies measured m/z.

highest docking scores (−6.214), followed by Vernolic acid (−4.995), Caffeic acid (−4.439), and 4-hydroxyphenyl acetic acid (−3.661), respectively. Moreover, Astragalin interacted with several important residues via H-bonds and aromatic hydrogen bond interactions with TRP9, HIS68, THR200, THR201, and Zinc1260 coordination, as shown in Figure 11. Interestingly, our docking results correlated well with the prediction of anti-cancer activity as described above.

Molecular Dynamic Simulation of *M. arboreus* Secondary Metabolites with the Carbonic Anhydrase IX (CA IX) Crystal Structure Using Desmond

To evaluate if the interactions highlighted in the docking poses are stable, we conducted detailed investigations using the molecular dynamic simulation tool in Maestro software. Our results showed that the complex was stable during the simulation time (100 ns), which was evident by stable RMSD values (Figure 12A). Moreover, Astragalin maintained various contacts

Table 1 The Predicted Bioactivity Scores of *M. arboreus* Secondary Metabolites Using PASS Online Webserver

Antineoplastic/ Anticarcinogenic Activity	Probability of Being Active (Pa)	Probability of Being Inactive (Pi)
Astragalin	0.953	0.001
4-hydroxyphenylacetic acid	0.403	0.030
Caffeic acid	0.571	0.014
Vernolic acid	0.464	0.055

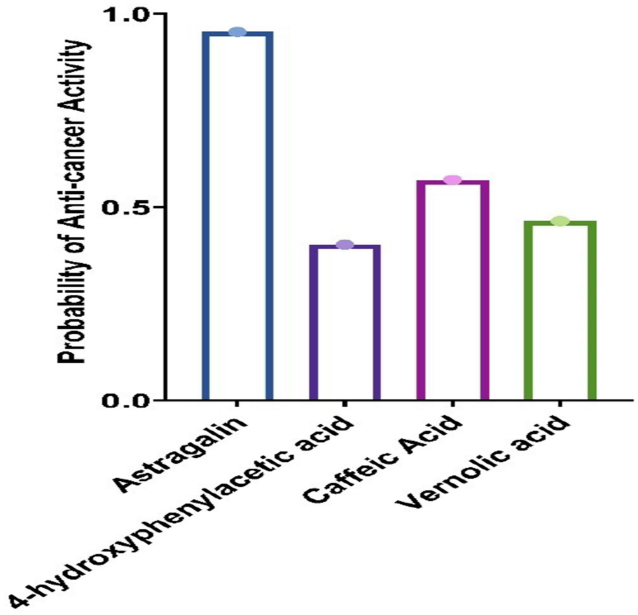

Figure 9 The probability of anti-cancer activity of *M. arboreus* secondary metabolites using PASS online webserver.

with amino acids, including HIS94, HIS96, GLU106, THR200, THR201, and THR202 for most of the simulation run. These interactions involved ionic, hydrogen, and hydrophobic interactions (Figure 12B). Moreover, the protein residue contacts with Astragalin were stable during a timescale of 100 ns, and Zinc 1260 coordination was maintained at 100% for the simulation run (Figure 12C), indicating stable and strong interactions between Astragalin and CA IX. Our docking and simulation data indicate the promising dual activity of Astragalin that could be mediated via CA IX inhibition.

Predictions of ADME Properties for the Secondary Bioactive Metabolites Identified in *M. arboreus* Extract

The physicochemical profile for the identified bioactive metabolites was predicted using two computational tools, and five important ADME parameters were evaluated. All metabolites demonstrated a molecular weight of less than 500 g/mol and exhibited low lipophilicity except for Vernolic acid, which demonstrated a log P of 5.10 (Table 4 and Figure 13). Additionally, the solubility correlated well with the lipophilicity in which all the metabolites were soluble except for

Table 2 The Predicted Biological Targets Involved in Mediating *Malvaviscus arboreus* Anti-Cancer Activity Using SWISS Target Prediction, Sea Search, and Molinspiration Web Servers

Compound Name	Target Predictions			
	SWISS Target Prediction	**SEA Search**	**Molinspiration**	
Astragalin	Carbonic anhydrase	Carbonic anhydrase	GPCR ligand Ion channel modulator Kinase inhibitor Nuclear receptor ligand Protease inhibitor Enzyme inhibitor	0.06 −0.05 0.10 0.20 −0.05 0.41
4-hydroxyphenyl acetic acid	Carbonic anhydrase	Carbonic anhydrase	GPCR ligand Ion channel modulator Kinase inhibitor Nuclear receptor-ligand Protease inhibitor Enzyme inhibitor	−0.53 −0.07 −1.02 −0.18 −0.69 −0.09

(*Continued*)

Table 2 (Continued).

Compound Name	Target Predictions			
	SWISS Target Prediction	**SEA Search**	**Molinspiration**	
Caffeic acid	Carbonic anhydrase	Carbonic anhydrase	GPCR ligand Ion channel modulator Kinase inhibitor Nuclear receptor-ligand Protease inhibitor Enzyme inhibitor	−0.48 −0.23 −0.81 −0.10 −0.79 −0.09
Vernolic acid	Cytochrome P450	Cannabinoid receptors	GPCR ligand Ion channel modulator Kinase inhibitor Nuclear receptor ligand Protease inhibitor Enzymeinhibitor	0.34 0.15 0.10 0.52 0.59 0.60

Vernolic acid, which had intermediate solubility. Regarding the BBB penetration, the two prediction tools showed distinct results. QikProp predicted that all the four metabolites are unable to cross BBB, while SWISS ADME predicted 4-hydroxyphenyl acetic acid and Vernolic acid can cross BBB. Moreover, Vernolic acid demonstrated the highest GI absorption (100%), followed by 4-hydroxyphenyl acetic acid (68%), Caffeic acid (54%), and Astragalin (11.9%), respectively. Among the four metabolites, only Astragalin violated hydrogen bond donor and acceptor rules for orally active drugs.

Cytochromes (CYP) P450 Enzymes Inhibition Profile for the Bioactive Metabolites Identified in *M. arboreus* Extract

Our computational predictions demonstrated that Astragalin, 4-hydroxyphenyl acetic acid, and Caffeic acid do not inhibit the five major CYP enzymes, CYP1A2, CYP2C19, CYP2C9, CYP2D6, and CYP3A4 (Table 5), while only Vernolic acid

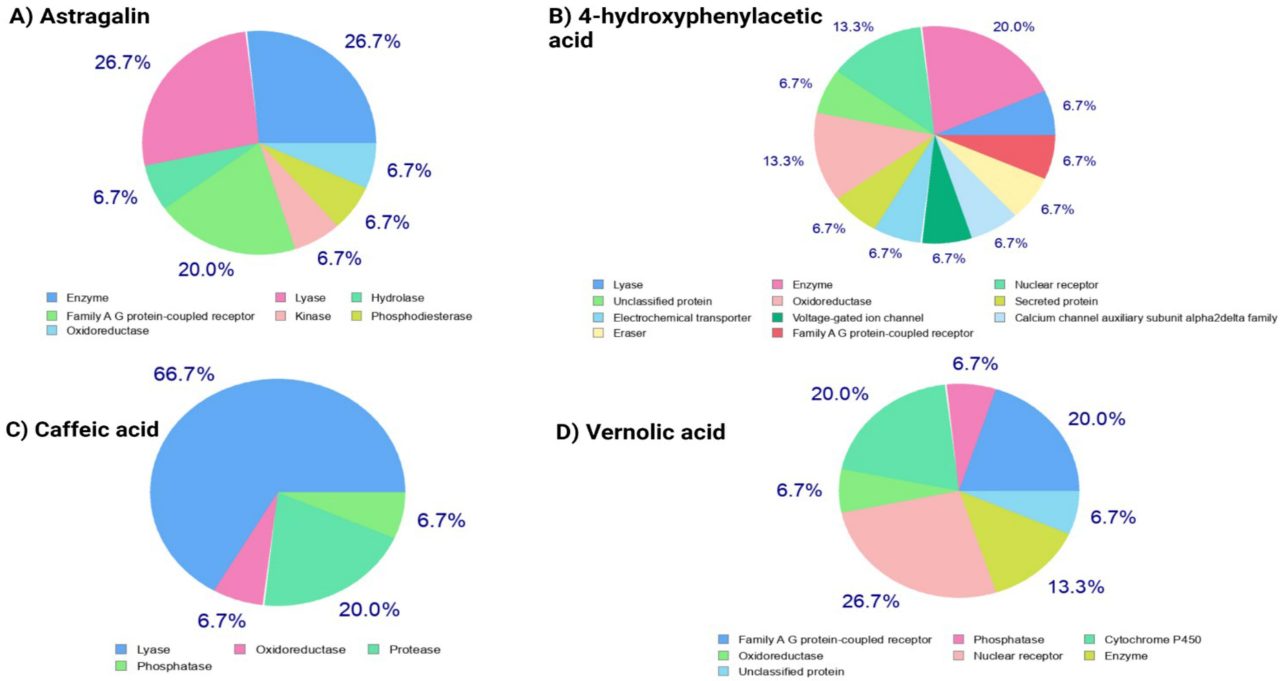

Figure 10 The target predictions for the secondary bioactive molecules identified in *M. arboreus* extract using Swiss target prediction. (**A**) Astragalin, (**B**) 4-hydroxyphenylacetic acid, (**C**) Caffeic acid, (**D**) Vernolic acid.

Table 3 The Docking Scores for the *M. arboreus* Metabolites with CA IX Using the Glide Tool

Compound Name	Glide Score	Interactions with Amino Acid Residues
Astragalin	−6.214	TRP9, HIS68, THR200, THR201, Zinc1260
4-hydroxyphenyl acetic acid	−3.661	HIS94, THR200, GOL1261, ZN1260
Caffeic acid	−4.439	Zinc1260
Vernolic acid	−4.995	THR200, Zinc1260

showed a predicted inhibition for CYP1A2, CYP2C9, and CYP2D6 enzymes. It is worth mentioning that none of the metabolites was predicted to inhibit the CYP3A4 enzyme that is involved in metabolizing several drug classes.

Organ Toxicity Predictions for the Bioactive Metabolites Identified in the *M. arboreus* Extract

The potential toxicity of the secondary bioactive metabolites was predicted using the ProTox-II online webserver. Among the predicted four metabolites, only Caffeic acid demonstrated 78% carcinogenicity (Table 6 and Figure 14), while the rest were inactive suggesting a safe and promising pharmaceutical profile for the identified metabolites.

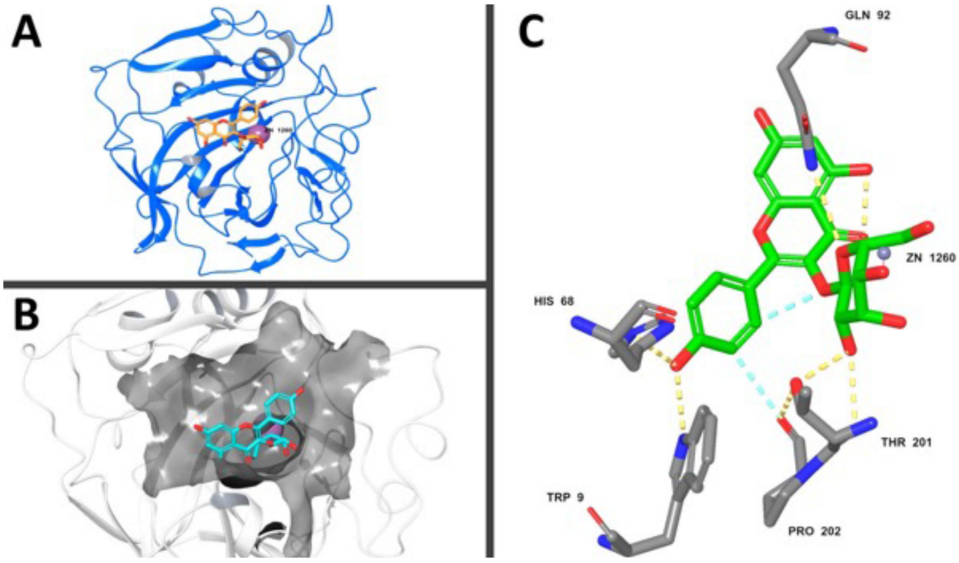

Figure 11 (**A**) Carbonic Anhydrase IX with Astragalin. (**B**) Astragalin occupies the binding pocket of CA IX using surface representation. (**C**) The molecular interactions of Astragalin with various amino acid residues in CA IX binding site (yellow color is H-bonds, and faded teal is aromatic hydrogen bond interaction).

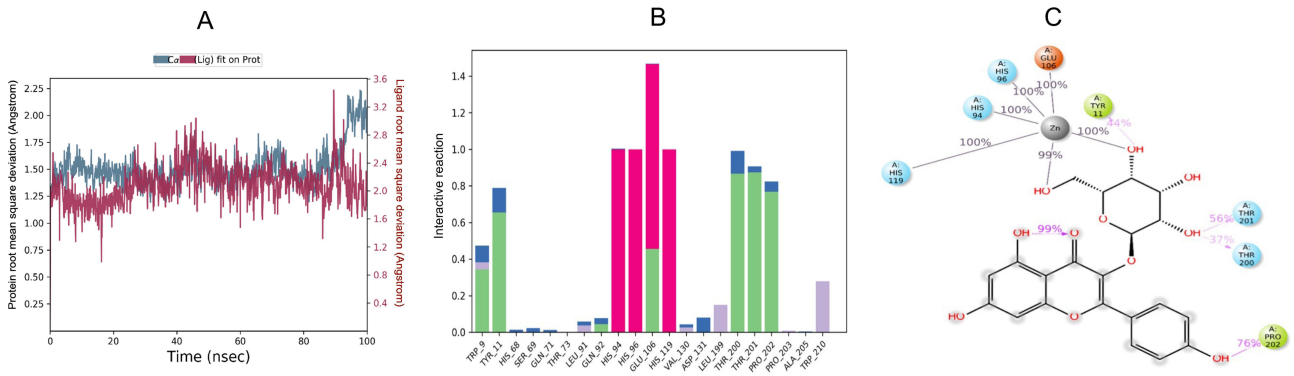

Figure 12 Simulation interaction diagram for Astragalin and CA IX complex for a timescale of 100 ns. (**A**) The protein and ligand RMSD graphs for Astragalin and CA IX complex for the timescale of 100 ns. (**B**) Astragalin and CA IX contacts for the timescale of 100 ns. Green (H-bonds), Purple (hydrophobic), Red (ionic), and blue (water bridge). (**C**) Astragalin and CA IX interactions for the timescale of 100 ns. Hydrogen bonds (purple), green (hydrophobic), and grey (metal coordination).

Table 4 The Predicted ADME Properties for the Secondary Metabolites Identified in *Malvaviscus arboreus* Extract Using SWISSADME and QikProp Tools

Compound Name	Molecular Weight		Log Po/w		Log S		BBB Permeant		GI Absorption		Rule of Five (ROF)
	SWISS ADME	QikProp	SWISS ADME	QikProp	SWISS ADME	QikProp	SWISS ADME	QikProp	SWISS ADME	QikProp	SWISSADME
Astragalin	448.38	448.382	−0.24	−0.823	−2.10 Soluble	−2.665	No	Inactive	Low	11.977	No; 2 violations: NorO>10, NHorOH>5
4-hydroxyphenyl acetic acid	152.15	152.149	1.02	1.253	−1.58 Soluble	−1.336	Yes	Inactive	High	68.076	Yes; 0 violation
Caffeic acid	180.16	180.16	1.09	0.531	−0.71 Soluble	−1.272	No	Inactive	High	54.11	Yes; 0 violation
Vernolic acid	296.44	296.449	5.10	4.948	−4.41 Moderately soluble	−5.369	Yes	Inactive	High	100	Yes; 0 violation

Discussion

M-AgNPs Properties

Change of the mixture ($AgNO_3$ and *M. arboreus* extract) color to brown suggested successful fabrication of well-distributed spherical M-AgNPs at nano-range that approved by DLS and TEM analysis which showed varied sizes. Since

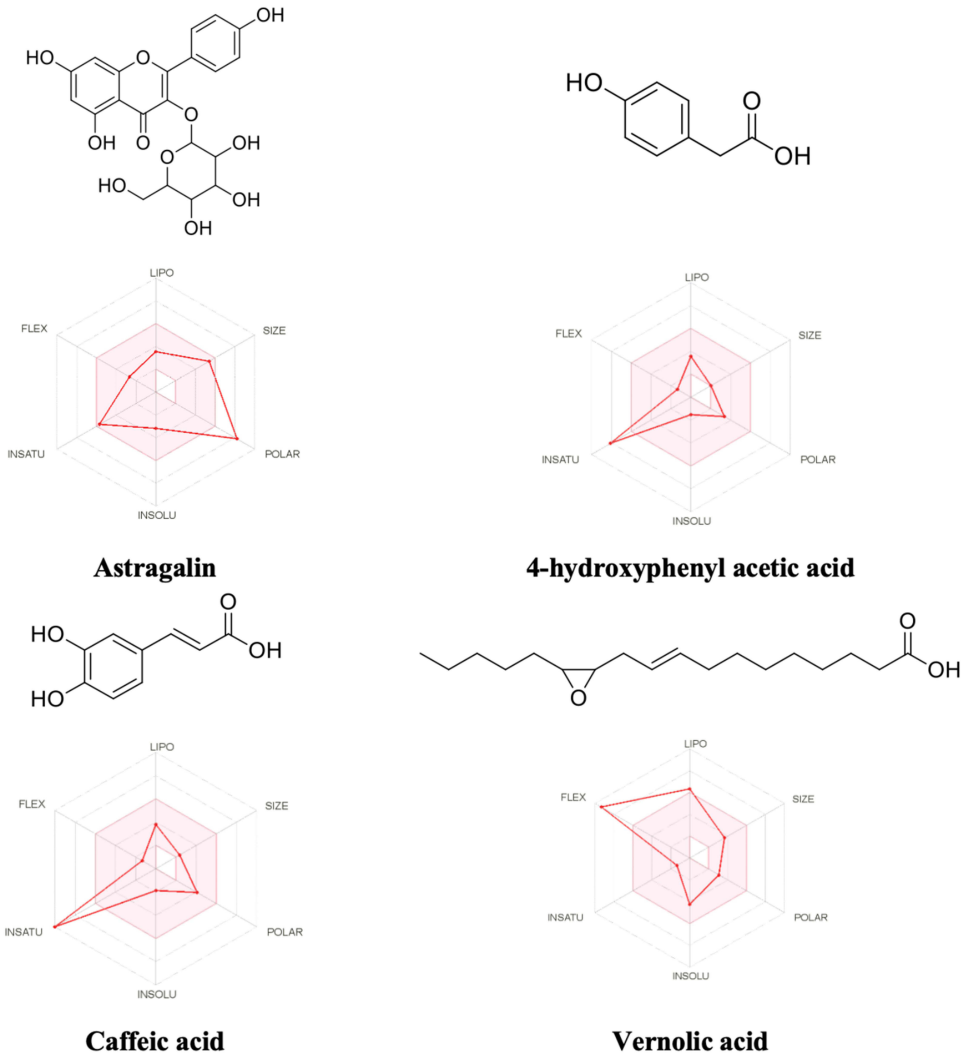

Figure 13 Prediction of the drug-likeness properties of the metabolites identified in *M. arboreus* extract using SWISSADME.

DLS analysis assesses the radius of the particles in an aqueous medium that may contain capping agents from the plant extract, TEM analysis is taken in dry conditions; therefore, variation in the size obtained by each technique is expected.[33,34] The PDI data indicated a monodispersed form of the M-AgNPs since its value is less than 3.[35] A similar trend of observation was also noted in a recent report.[36] Negative zeta potential indicates repulsion among the particles, which confirms long-term NPs stability.[37] The negative potential values might be related to the organic molecules from the plant extract that cap the NPs. A recent study by Sharifi-Rad et al[38] also had a negative zeta potential (−25.2 mV) for the AgNPs prepared from *Otostegia persica* Leaf Extract.

Additionally, the EDX spectrum of AgNPs confirmed the existence of O and C peaks indicating the occurrence of carbon-based compound and phytochemicals that act as stabilizing agents in NP formation. Besides, the existence of C could be related to the carbon type used to mount the anticipated sample throughout the experiment, where the O might indicate the surface oxidation state.[39] The significant role of phytochemicals in AgNPs fabrication as reducing and capping agents is widely studied, however, varied within plants, which could be related to specific plant metabolites. Proteins and polyphenolics in the plant extract and the M-AgNPs solution were noted; however, peaks observed from the plant extract were slightly shifted in the M-AgNPs solution indicating the role of phytochemicals in the reduction process. The major noted peaks were related to OH groups of polyphenolic and N-H stretching of amines that were clear at a range near 3300 cm^{-1} and peaks for carbonyl (C = O) stretching of proteins and amide 1 that were reported at 1635 cm^{-1} for the plant extract and M-AgNPs.[20,40]

M-AgNPs Biological Activity

Our results identified that the M-AgNPs exerted significant anti-bacterial activity on both gram-positive and gram-negative bacteria, and the ampicillin conjugate typically caused synergistic effect on their activity. A previous study reported the synergistic effect of AgNPs when combined with antibiotics,[41] but in this case, the AgNPs were created in solution using an electro-colloidal system.[42] However, our previous studies showed more aggregation of the antibiotic conjugate green-AgNPs, which appeared to have an antagonistic effect.[9,43] The plant extract had the least antimicrobial potential; however, a previous study reported that combining plant extracts with traditional antibiotics exerts synergistic or additive antibiotic effects.[44] In our case, it would have been useful to combine the *M. arboreus* extract with ampicillin to check for a similar pharmacological response.

Table 5 The CYP-P450 Enzyme Inhibition Profile for the Bioactive Molecules Identified in *M. arboreus* Extract Using SWISSADME

Compound	CYP1A2	CYP2C19	CYP2C9	CYP2D6	CYP3A4
Astragalin	No	No	No	No	No
4-hydroxyphenyl acetic acid	No	No	No	No	No
Caffeic acid	No	No	No	No	No
Vernolic acid	Yes	No	Yes	Yes	No

Table 6 Organ and Endpoint Toxicity Predicted Using ProTox-II

Compound Name	Classification				
	Organ Toxicity (% Probability)	Toxicity Endpoint (% Probability)			
	Hepatotoxicity	Carcinogenicity	Immunotoxicity	Mutagenicity	Cytotoxicity
Astragalin	Inactive (82)	Inactive (85)	Inactive (64)	Inactive (76)	Inactive (69)
4-hydroxyphenyl acetic acid	Inactive (55)	Inactive (74)	Inactive (99)	Inactive (94)	Inactive (83)
Caffeic acid	Inactive (57)	Active (78)	Inactive (50)	Inactive (98)	Inactive (86)
Vernolic acid	Inactive (66)	Inactive (62)	Inactive (98)	Inactive (84)	Inactive (64)

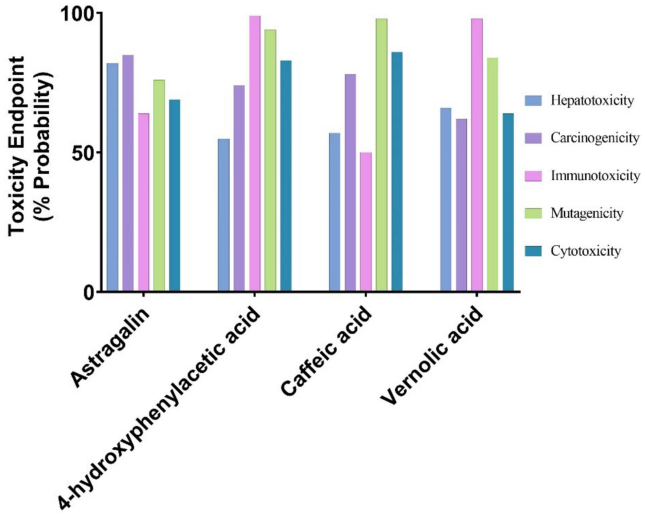

Figure 14 Organ and endpoint toxicity predictions for *M. arboreus* secondary metabolites using ProTox-II.

The gram-positive *S. aureus* was more susceptible to the effects of the M-AgNPs than the other tested bacteria, and expectedly, the combination of the M-AgNPs with ampicillin had a greater impact on this strain than the other tested strains. A greater increase in efficacy of ampicillin conjugated NPs was noted compared to ampicillin alone and other tested agents. This represents a viable option for the treatment of MRSA. Both gram-negative bacteria, *E. coli*, and *K. pneumoniae*, were the least affected by the treatments, although gram-negative bacteria may be more susceptible to silver nanoparticles.[41] Another study also showed *Lycium shawii*-AgNPs to have a greater anti-microbial capacity on the gram-positive *S. aureus* bacteria.[9] Gram-negative bacteria can be more resistant to certain antibiotics because of the features and functions of the outer membrane.[45] A possible explanation could be due to the outer membrane of the gram-negative bacteria, which contains LPS, which is a cause of virulence, but also could lead to the binding of plant metabolites to this structure and not allow penetration or even repelling the particles, depending on the functional groups of the metabolites present around the nanoparticle itself. These theories are supported by the fact that certain plant secondary metabolites bind strongly to the LPS,[46] and other plant metabolites do not bind but rather repel specific microbes.[47] A further detailed examination using microscopy techniques would help in explaining the observations.

Cytotoxicity data reveal that M-AgNPs had a potent effect on HCT113 colon cancer cells and very little on the MDA-MB-231 ER+ positive breast cancer cells. It is important to note that credible cytotoxic effects occurred on the normal breast epithelial cell line, which indicates a lack of therapeutic specificity at least in the case of this particular breast cancer. In the field of drug discovery, it is essential to perform toxicity studies before implying a therapeutic role on a new drug candidate. The toxicity studies may start from in silico studies and expand to in vitro and in vivo studies using a large panel of cells, general toxicity on animals, and finally, in humans. After deciphering these effects, treatments for diseases along with doses can be stipulated. Therefore, more extensive studies are needed to determine its value and use in colon carcinoma by the initial utilization of an array of normal and cancerous cell lines.

Nevertheless, the data generated here agree with the in silico biological activities of the secondary metabolites of *M. arboreus*. Since, the crude extract from which the M-AgNPs have been prepared have all the metabolites identified from the mass spectrophotometric data; we expect that the differences observed in cell cytotoxic response are related to different metabolites in action exerting cytotoxicity by distinguished mechanisms. Furthermore, cellular differences in cytotoxic response are also likely to be governed by the cell texture, which refers to the cellular environment, cell type, genomic and proteomic characteristics, and passage of the individual cell. Thus, using crude extracts of plant material presents an opportunity of broadening the therapeutic application.

Plant secondary metabolites tend to have very specific functions,[48] evolutionarily developed due to the real-life need to continue to grow and survive. The specific functions are attributed to a high degree of selectivity towards its biological targets having less promiscuity than traditional man-made synthetic drugs.[49] The specificities and function are dictated by

the biochemical properties of the structure and their functional groups. Standard AgNPs are known to have cytotoxic properties in vitro,[50] but with green synthesis, therapeutic secondary plant metabolites surrounding the silver nucleus can lead to additional properties[51] and possibly a targeted approach that leads to selectivity towards certain types of diseased cells, broadening the safety index and the therapeutic implications of the treatment possibly contributing to precision medicine. Thus, it is reasonable to assume that it is the functional groups present in the secondary metabolites surrounding the NPs that dictate the cytotoxic activity, selectivity, and safety profile. Many studies show the cytotoxic activity of plant green synthesized AgNPs on cancer cells.[9,43,52] However, our study is the first to test the anti-cancer activity of *M. arboreus* and the *M. arboreus* AgNPs.

M. arboreus Metabolites

Varied metabolites were detected from the aqueous extract of *M. arboreus* that showed cytotoxic, antioxidant and anti-inflammatory effects. The flavonoid Astragalin is also known as kaempferol-3-*O*-b-d-glucoside. It has been isolated from many different types of plants and from within families such as *Convolvulaceae, Fabaceae* and *Eucommiaceae*.[53] It has broad anti-inflammatory properties suppressing NFKB signals, reducing inflammatory cells and attenuating the expression of TNF-a, IL-6, and IL-1b as well as myeloperoxidase.[54] In addition, it is reported to have effects on other enzymes such as metalloproteinases, cyclooxygenase, inducible nitric oxide synthase (iNOS), and kinases and regulates proteins involved in apoptosis and autophagy, such as caspases, Bax and Bcl2, in addition, alters the expression levels of many inflammatory cytokines.[53] The link between reactive oxygen species (ROS) generation and the regulation of autophagy and the initiation and progression of cancers is well established.[55] Myeloperoxidase (MPO) catalyzes the formation of various types of ROS, which contributes to tissue damage stress responses and malfunctioned autophagy, all of which contribute to switching of cellular responses leading to oncogenic effects. Furthermore, silencing of MPO and iNOS led to increased apoptosis, thus acting as a redox switch to regulate programmed cell death[56] and, as such, regulating ROS is considered a useful strategy for cancer treatment. It is important to note that carbonic anhydrase IX is a hypoxia-induced protein, an acid-base regulator, and a driver of tumorigenesis. Key to the pathogenic effect of CA IX is the fact that ROS promotes a hypoxic state by destabilizing the mitochondrial electron transport chain and subsequently causing a vicious loop where mitochondrial hypoxia further drives ROS production.[57] Since we found Astragalin to bind strongly to the CA IX, it could be stipulated that the in vitro cytotoxic effect of *M. arboreus* on breast cancer and colon cancer cells is likely to be occurring through a faceted signaling process, where a reduction of ROS occurs, dominated by anti-inflammatory effects, and a switch to the normal repair mode promoting clean-up, autophagy, and apoptosis. Other studies have also shown medicinal plants to bind to the CA IX enzyme and regulate ROS production in macrophages.[8,9]

4-hydroxyphenyl acetic acid (4-HPA) is a polyphenol having antioxidant action and was shown to protect against paracetamol-induced liver damage by enhancing the activity of antioxidant enzymes and increasing Phase II metabolism. As such, it could be used as a naturally occurring plant-based hepatoprotective agent.[58] Furthermore, 4-HPA was able to reduce inflammation and expression of hypoxia-induced HIF-1a protein.[59] HIF-1a is overexpressed in many different cancers, and its activity is linked to the induction of CA IX,[60] oncogenesis, and cancer progression.[61] This agrees with results from our in silico studies, which also indicate 4-HPA to bind to CA IX. Furthermore, 4-HPA also has antimicrobial potential. Its antimicrobial efficacy was proved on *Listeria monocytogenes,*[62] and derivatives of 4-HPA had microbial effects on *Bacillus coagulans, Geobacillus stearothermophilus*, and *Alcaligenes faecalis*.[63]

Caffeic acid is a phenolic compound found in abundance in fruits, oils, teas, coffee, wine, and in some plants such as propolis. It has antioxidant, anti-inflammatory, and anti-cancer properties, attributed to its ability to attenuate ROS formation, induce DNA oxidation of cancer cells, and prevent tumor cell angiogenesis.[64] Furthermore, it is known to have anti-cancer activity against various cancer cells, such as oral cancer, lung cancer, cervical cancer, and liver cancer. It also attenuated the growth of both ER+ and ER-Breast cancer cells, MDA MB 231 and MCF-7, by hindering ER/cyclin D1 and IGF-IR/pAKt signaling pathways, thus preventing cancer cell proliferation.[65] In colon cancer, caffeic acid had a potent effect inducing apoptosis via enhanced AMPK activation; another mechanism could also be through inhibition of the Akt and mTOR pathway and the ERK/MEK1 pathway.[66] Caffeic acid has anti-microbial effects against several strains of *staphylococcus aureus* and provides synergistic effects when combined with traditional antibiotics, erythromycin, clindamycin, and cefoxitin.[44]

Vernolic acid, also known as leukotoxin, is a plant long-chain monounsaturated epoxy fatty acid. Vernolic acid also has cytotoxic properties on cancer cells. Plant fatty acids and fatty acids in general have shown cytotoxic potential[67] against breast cancer cells, MDA MB 231.[68] Although higher levels of leukotoxin are known to cause strong toxicity, possibly by disrupting the functional effects of the endothelial barrier.[69] Our in silico data predicts vernolic acid to be an inhibitor of 4 out of the 5 tested CYP450 enzymes, and since leukotoxins are known to be formed by cytochrome P450 enzymes,[69] our predictions on the inhibitory effect of CYP450 enzymes is expected. Fatty acids are also known to have antimicrobial activity, exerting their effects in several ways, such as destabilizing bacterial membranes and interfering with bacterial metabolic processes.[70]

In silico Evaluation of *M. arboreus* Metabolites Pharmacological Properties

In this study, the biological evaluation of the *M. arboreus* extract demonstrated promising anti-cancer and anti-bacterial activities using in-vitro testing. Thus, several computational tools were utilized to investigate the anti-cancer activity, molecular targets, ADME properties, CYP inhibition, and organ toxicity. Interestingly, among the evaluated metabolites, Astragalin demonstrated the highest anti-cancer probability that could be mediated via CA IX, which was predicted using three web servers. Additionally, these results were further confirmed using molecular docking that showed Astragalin possesses the highest docking score with a comparatively greater number of multiple interactions. Our docking results were further confirmed using a deeper investigation molecular dynamic tool for Astragalin and CA IX complex. The simulation findings suggest that interactions between Astragalin and CA IX were stable over the simulation run, indicating stable and consistent interactions between Astragalin and CA IX enzyme, which was of particular interest.

Considering the promising docking and simulation results, it was necessary to evaluate the physicochemical properties and safety profile of the identified metabolites. Our findings suggest that all the metabolites possess acceptable pharmaceutical properties, in particular, Lipinski's rule of five, except for Astragalin; further development to enhance Astragalin's oral bioavailability would be needed, or it could be considered for parenteral use. All the metabolites showed good safety profiles regarding CYP inhibition and organ toxicity. Our data point out the promising dual anti-cancer and anti-bacterial actions for *M. arboreus* extract that were mediated via CA IX inhibition and validated using in-vitro and in-silico methods.

Summary and Conclusion

M. arboreus is a well-known herb that has been used for centuries for several ailments. *M. arboreus* contains several bioactive secondary metabolites that may contribute significantly to M-AgNPs fabrication, cytotoxic and antibacterial effects. In particular, Astragalin presents as a secondary plant metabolite with therapeutic implications for several diseases targeting carbonic anhydrase IX. As predicted, these metabolites have a good safety profile. Therefore, *M. arboreus* appears to be a strong candidate for targeting processes that facilitate neoplastic growth, such as hypoxia, angiogenesis, ROS generation, and autophagy. In the current study, we elucidated its anti-neoplastic potential and antibacterial effects whilst highlighting the ability to use plant-based biogenic AgNPs as a valuable tool in producing selective and targeted therapeutics for use in precision medicine. The biochemical properties of the secondary metabolites dictate their pharmacology and ability to target and repel various biological structures. hence providing a mechanism of selectivity presumably and consequently ablating toxicity. Although much more research is required in this field, this presents an opportunity for utilizing plant-based AgNP synthesis for further research and development in targeting and treating specific cancers and bacterial infections and hence may be valuable in developing precision medicine.

Data Sharing Statement

Data will be available upon request to the corresponding author.

Acknowledgments

The authors extend their appreciation to Ahlam Hamad Abdullah Alrokban and Nada Ibrahim Abdullah Alsugiran, Jumana M. Ghannam, Mona Alanazi, Department of biology, Faculty of Science, and Dhuha Fahad AlSuwaid, Health

Science Research Center, Princess Nourah bint Abdulrahman University, for their technical support during the experimental period of this work.

Funding

This work was funded by the Deanship of Scientific Research at Princess Nourah bint Abdulrahman University, through the Research Groups Program Grant no. (RGP-1443-0041).

Disclosure

The authors declare no conflicts of interest in this work.

References

1. Jarvie H, King S, Dobson P. Nanoparticle. In: Gregersen E, Rogers K, editors. *Encyclopedia Britannica*. Britannica; 2019. Available from: https://www.britannica.com/science/nanoparticle/additional-info#contributors.
2. Morozova YA, Dergachev DS, Subotyalov MA. Silver nanoparticles: safety and efficiency for human health. *Rev Clin Pharmacol Drug Ther*. 2021;19(3):247–257. doi:10.17816/RCF193247-257
3. Alwan SH, Alwan H, Al-Saeed MH, Abid HA. Safety assessment and biochemical evaluation of the effect of biogenic silver nanoparticles (using bark extract of C. zeylanicum) on Rattus norvegicus rats. *Baghdad J Biochem Appl Biol Sci*. 2021;2(03):133–145. doi:10.47419/bjbabs.v2i03.67
4. Lambré C, Barat Baviera JM, Bolognesi C, et al. Safety assessment of the substance silver nanoparticles for use in food contact materials. *EFSA J*. 2021;19(8). doi:10.2903/J.EFSA.2021.6790
5. Iravani S, Korbekandi H, Mirmohammadi S, Zolfaghari B. Synthesis of silver nanoparticles: chemical, physical and biological methods. *Res Pharm Sci*. 2014;9(6):385.
6. Pal G, Rai P, Pandey A. Green synthesis of nanoparticles: a greener approach for a cleaner future. In: *Green Synthesis, Characterization and Applications of Nanoparticles*. Elsevier; 2019:1–26. doi:10.1016/B978-0-08-102579-6.00001-0
7. Ahmed S, Ahmad M, Swami BL, Ikram S. A review on plants extract mediated synthesis of silver nanoparticles for antimicrobial applications: a green expertise. *J Adv Res*. 2016;7(1):17–28. doi:10.1016/J.JARE.2015.02.007
8. Suliman RS, Alghamdi SS, Ali R, et al. The role of myrrh metabolites in cancer, inflammation, and wound healing: prospects for a multi-targeted drug therapy. *Pharmaceuticals*. 2022;15(8):944. doi:10.3390/PH15080944
9. Mohammed AE, Ameen F, Aabed K, et al. In-silico predicting as a tool to develop plant-based biomedicines and nanoparticles: Lycium *shawii* metabolites. *Biomed Pharmacother*. 2022;150:113008. doi:10.1016/j.biopha.2022.113008
10. Talank N, Morad H, Barabadi H, et al. Bioengineering of green-synthesized silver nanoparticles: in vitro physicochemical, antibacterial, biofilm inhibitory, anticoagulant, and antioxidant performance. *Talanta*. 2022;243:123374. doi:10.1016/J.TALANTA.2022.123374
11. Suliman RS, Alghamdi SS, Ali R, et al. Distinct mechanisms of cytotoxicity in novel nitrogenous heterocycles: future directions for a new anti-cancer agent. *Molecules*. 2022;27(8):2409. doi:10.3390/MOLECULES27082409
12. Hesham O, Refaat J, Ramadan Abdelmohsen U, et al. Botanical studies of leaves of Malvaviscus arboreus Cav. family: Malvaceae, cultivated in Egypt. *J Pharmacogn Phytochem*. 2017;6(3):149–153.
13. Lim TK. *Edible Medicinal and Non-Medicinal Plants*. Vol. 1. Springer; 2012.
14. Mustarichie R, Wicaksono IA, Hayati C. Anti-alopecia characteristics of ethanol extract, n-hexane, ethyl acetate and water fractions of Malvaviscus arboreus Cav. *Res J Pharm Technol*. 2018;11(11):5066–5072. doi:10.5958/0974-360X.2018.00924.1
15. Abdelhafez OH, Fawzy MA, Fahim JR, et al. Hepatoprotective potential of Malvaviscus arboreus against carbon tetrachloride-induced liver injury in rats. *PLoS One*. 2018;13(8):e0202362. doi:10.1371/JOURNAL.PONE.0202362
16. Campos-Vidal Y, Herrera-Ruiz M, Trejo-Tapia G, Gonzalez-Cortazar M, Aparicio AJ, Zamilpa A. Gastroprotective activity of kaempferol glycosides from Malvaviscus arboreus Cav. *J Ethnopharmacol*. 2021;268. doi:10.1016/J.JEP.2020.113633
17. Rodríguez-García CM, Ruiz-Ruiz JC, Peraza-Echeverría L, et al. Antioxidant, antihypertensive, anti-hyperglycemic, and antimicrobial activity of aqueous extracts from twelve native plants of the Yucatan coast. *PLoS One*. 2019;14(3):e0213493. doi:10.1371/JOURNAL.PONE.0213493
18. Abdelhafez OH, Othman EM, Fahim JR, et al. Metabolomics analysis and biological investigation of three Malvaceae plants. *Phytochem Anal*. 2020;31(2):204–214. doi:10.1002/PCA.2883
19. Yeasmin Z, Tanvir S, Sharmin T, Bin Rashid R, Al Amin Sikder M, Rashid MA. Bioactivities of Malvaviscus arboreus var. drummondii and phyllanthus reticulatus poir; 2014. Available from: http://www.novapdf.com. Accessed March 21, 2023.
20. Dasari S, Suresh KA, Rajesh M, et al. Biosynthesis, characterization, antibacterial and antioxidant activity of silver nanoparticles produced by lichens. *J Bionanosci*. 2013;7(3):237–244. doi:10.1166/jbns.2013.1140
21. Mie R, Samsudin MW, Din LB, Ahmad A, Ibrahim N, Adnan SNA. Synthesis of silver nanoparticles with antibacterial activity using the lichen Parmotrema praesorediosum. *Int J Nanomedicine*. 2014;9:121. doi:10.2147/IJN.S52306
22. Siddiqi KS, Rashid M, Rahman A, Husen A, Rehman S, Rehman S. Biogenic fabrication and characterization of silver nanoparticles using aqueous-ethanolic extract of lichen (Usnea longissima) and their antimicrobial activity. *Biomater Res*. 2018;22(1):1–9. doi:10.1186/s40824-018-0135-9
23. Paul S, Singh ARJ, Sasikumar CS. Green synthesis of bio-silver nanoparticles by Parmelia perlata, Ganoderma lucidum and Phellinus igniarius & their fields of application. *Indian J Res Pharma Biotechnol*. 2015;5674:100–110.
24. Wayne PA. Clinical and Laboratory Standards Institute: performance standards for antimicrobial susceptibility testing: 20th informational supplement. In: *CLSI Document M100-S20*. CLSI; 2010.
25. Fan Y, Gonzales AA, Gonzales AA, Fenniri H. Enhanced antibiotic activity of ampicillin conjugated to gold nanoparticles on PEGylated rosette nanotubes. *International Journal of Nanomedicine*. 2019;14:7281–7289. doi:10.2147/IJN.S209756
26. Filimonov DA, Lagunin AA, Gloriozova TA, et al. Prediction of the biological activity spectra of organic compounds using the pass online web resource. *Chem Heterocycl Compd*. 2014;50(3):444–457. doi:10.1007/s10593-014-1496-1

27. Gfeller D, Grosdidier A, Wirth M, Daina A, Michielin O, Zoete V. SwissTargetPrediction: a web server for target prediction of bioactive small molecules. *Nucleic Acids Res*. 2014;42:W32–W38. doi:10.1093/NAR/GKU293
28. Ertl P, Bienfait B. Calculation of molecular properties and bioactivity score; 2022. Available from: https://www.molinspiration.com/cgi-bin/properties. Accessed August 20, 2022.
29. Friesner RA, Banks JL, Murphy RB, et al. Glide: a new approach for rapid, accurate docking and scoring. 1. Method and assessment of docking accuracy. *J Med Chem*. 2004;47(7):1739–1749. doi:10.1021/JM0306430
30. Daina A, Michielin O, Zoete V. SwissADME: a free web tool to evaluate pharmacokinetics, drug-likeness and medicinal chemistry friendliness of small molecules. *Sci Rep*. 2017;7(1):1–13. doi:10.1038/srep42717
31. Banerjee P, Eckert AO, Schrey AK, Preissner R. ProTox-II: a webserver for the prediction of toxicity of chemicals. *Nucleic Acids Res*. 2018;46:W257. doi:10.1093/NAR/GKY318
32. Hesham Abdelhafez O, Refaat Fahim J, Ramadan Abdelmohsen U, et al. Headspace volatiles of the leaves and flowers of Malvaviscus arboreus Cav. (Malvaceae). *J Mex Chem Soc*. 2021;65(1):141–148. doi:10.29356/JMCS.V65I1.1431
33. Bhattacharjee S. DLS and zeta potential – what they are and what they are not? *J Control Release*. 2016;235:337–351. doi:10.1016/J.JCONREL.2016.06.017
34. Fan X, Zheng W, Singh DJ. Light scattering and surface plasmons on small spherical particles. *Light Sci Appl*. 2014;3(6):e179–e179. doi:10.1038/lsa.2014.60
35. Manosalva N, Tortella G, Cristina Diez M, et al. Green synthesis of silver nanoparticles: effect of synthesis reaction parameters on antimicrobial activity. *World J Microbiol Biotechnol*. 2019;35(6). doi:10.1007/S11274-019-2664-3
36. Mohammed AE, Alghamdi SS, Alharbi NK, et al. Limoniastrum monopetalum–mediated nanoparticles and biomedicines: in silico study and molecular prediction of biomolecules. *Molecules*. 2022;27(22):8014. doi:10.3390/MOLECULES27228014
37. Kordy MGM, Abdel-Gabbar M, Soliman HA, et al. Phyto-capped Ag nanoparticles: green synthesis, characterization, and catalytic and antioxidant activities. *Nanomaterials*. 2022;12(3):373. doi:10.3390/NANO12030373
38. Sharifi-Rad M, Pohl P, Epifano F. Phytofabrication of silver nanoparticles (AgNPs) with pharmaceutical capabilities using Otostegia persica (Burm.) boiss. leaf extract. *Nanomaterials*. 2021;11(4):1045. doi:10.3390/NANO11041045
39. Ameen F. Optimization of the synthesis of fungus-mediated bi-metallic Ag-Cu nanoparticles. *Appl Sci*. 2022;12(3):1384. doi:10.3390/APP12031384/S1
40. Khandel P, Kumar Shahi S, Kanwar L, Kumar Yadaw R, Kumar Soni D. Biochemical profiling of microbes inhibiting Silver nanoparticles using symbiotic organisms. *Int J Nano Dimension*. 2018;9(3):273–285.
41. Dakal TC, Kumar A, Majumdar RS, Yadav V. Mechanistic basis of antimicrobial actions of silver nanoparticles. *Front Microbiol*. 2016;7:1831. doi:10.3389/FMICB.2016.01831
42. de Souza A, Mehta D, Leavitt RW, Leavitt RW. Bactericidal activity of combinations of silver–water dispersion TM with 19 antibiotics against seven microbial strains. *Curr Sci*. 2006;10:926–929.
43. Mohammed AE, Al-Keridis LA, Rahman I, et al. Silver nanoparticles formation by Jatropha integerrima and LC/MS-QTOF-based metabolite profiling. *Nanomaterials*. 2021;11(9):2400. doi:10.3390/NANO11092400
44. Kępa M, Miklasińska-Majdanik M, Wojtyczka RD, et al. Antimicrobial potential of caffeic acid against Staphylococcus aureus clinical strains. *Biomed Res Int*. 2018;2018:1–9. doi:10.1155/2018/7413504
45. Breijyeh Z, Jubeh B, Karaman R. Resistance of gram-negative bacteria to current antibacterial agents and approaches to resolve it. *Molecules*. 2020;25(6):1340. doi:10.3390/MOLECULES25061340
46. Delehanty JB, Johnson BJ, Hickey TE, Pons T, Ligler FS. Binding and neutralization of lipopolysaccharides by plant proanthocyanidins. *J Nat Prod*. 2007;70(11):1718–1724. doi:10.1021/NP0703601
47. Pang Z, Chen J, Wang T, et al. Linking plant secondary metabolites and plant microbiomes: a review. *Front Plant Sci*. 2021;12:300. doi:10.3389/FPLS.2021.621276/BIBTEX
48. Böttger A, Vothknecht U, Bolle C, Wolf A. Plant secondary metabolites and their general function in plants. In: *Lessons on Caffeine, Cannabis & Co: Plant-Derived Drugs and Their Interaction with Human Receptors*. 2018:3–17. Doi:10.1007/978-3-319-99546-5_1
49. Lahlou M. The success of natural products in drug discovery. *Pharmacol Pharm*. 2013;2013(03):17–31. doi:10.4236/PP.2013.43A003
50. Rakowski M, Porębski S, Grzelak A. Silver nanoparticles modulate the epithelial-to-mesenchymal transition in estrogen-dependent breast cancer cells in vitro. *Int J Mol Sci*. 2021;22:17. doi:10.3390/IJMS22179203
51. Asif M, Yasmin R, Asif R, Ambreen A, Mustafa M, Umbreen S. Green synthesis of silver nanoparticles (AgNPs), structural characterization, and their antibacterial potential. *Dose-Response*. 2022;20(2):1–11. doi:10.1177/15593258221088709
52. Mohammed AE, Al-Megrin WA. Biological potential of silver nanoparticles mediated by Leucophyllum frutescens and Russelia equisetiformis extracts. *Nanomaterials*. 2021;11(8):2098. doi:10.3390/NANO11082098
53. Riaz A, Rasul A, Hussain G, et al. Astragalin: a bioactive phytochemical with potential therapeutic activities. *Adv Pharmacol Sci*. 2018;2018. doi:10.1155/2018/9794625
54. Shukla R, Pandey V, Vadnere GP, Lodhi S. Role of flavonoids in management of inflammatory disorders. In: *Bioactive Food as Dietary Interventions for Arthritis and Related Inflammatory Diseases*. Academic Press; 2019:293–322. doi:10.1016/B978-0-12-813820-5.00018-0
55. Azad MB, Chen Y, Gibson SB. Regulation of autophagy by reactive oxygen species (ROS): implications for cancer progression and treatment. *Antioxid Redox Signal*. 2009;11(4):777–790. doi:10.1089/ARS.2008.2270
56. Saed GM, Ali-Fehmi R, Jiang ZL, et al. Myeloperoxidase serves as a redox switch that regulates apoptosis in epithelial ovarian cancer. *Gynecol Oncol*. 2010;116(2):276–281. doi:10.1016/J.YGYNO.2009.11.004
57. Tafani M, Sansone L, Limana F, et al. The interplay of reactive oxygen species, hypoxia, inflammation, and sirtuins in cancer initiation and progression. *Oxid Med Cell Longev*. 2016;2016:1–18. doi:10.1155/2016/3907147
58. Zhao H, Jiang Z, Chang X, Xue H, Yahefu W, Zhang X. 4-hydroxyphenylacetic acid prevents acute APAP-induced liver injury by increasing phase II and antioxidant enzymes in mice. *Front Pharmacol*. 2018;9:653. doi:10.3389/FPHAR.2018.00653/BIBTEX
59. Liu Z, Xi R, Zhang Z, et al. 4-hydroxyphenylacetic acid attenuated inflammation and edema via suppressing HIF-1α in seawater aspiration-induced lung injury in rats. *Int J Mol Sci*. 2014;15(7):12861. doi:10.3390/IJMS150712861

60. Sowa T, Menju T, Chen-Yoshikawa TF, et al. Hypoxia-inducible factor 1 promotes chemoresistance of lung cancer by inducing carbonic anhydrase IX expression. *Cancer Med*. 2017;6(1):288–297. doi:10.1002/CAM4.991
61. Semenza GL. Defining the role of hypoxia-inducible factor 1 in cancer biology and therapeutics. *Oncogene*. 2010;29(5):625. doi:10.1038/ONC.2009.441
62. YujiaLiu SC, Zhang G, Zhang G, et al. Antimicrobial mechanism of 4-hydroxyphenylacetic acid on Listeria monocytogenes membrane and virulence. *Biochem Biophys Res Commun*. 2021;572:145–150. doi:10.1016/J.BBRC.2021.07.096
63. Sari M, Chung Y, Agatha F, Kwoun Kim H. Evaluation of antioxidant and antimicrobial activity of phenolic lipids produced by the transesterification of 4-hydroxyphenylacetic acid and triglycerides. *Appl Biol Chem*. 2019;62:5. doi:10.1186/s13765-019-0419-3
64. Monteiro Espíndola KM, Ferreira RG, Mosquera Narvaez LE, et al. Chemical and pharmacological aspects of caffeic acid and its activity in hepatocarcinoma. *Front Oncol*. 2019;9:541. doi:10.3389/FONC.2019.00541/BIBTEX
65. Rosendahl AH, Perks CM, Zeng L, et al. Caffeine and caffeic acid inhibit growth and modify estrogen receptor and insulin-like growth factor I receptor levels in human breast cancer. *Clin Cancer Res*. 2015;21(8):1877–1887. doi:10.1158/1078-0432.CCR-14-1748
66. Alam M, Ahmed S, Elasbali AM, et al. Therapeutic implications of caffeic acid in cancer and neurological diseases. *Front Oncol*. 2022;12:634. doi:10.3389/FONC.2022.860508/BIBTEX
67. Jóźwiak M, Filipowska A, Fiorino F, Struga M. Anticancer activities of fatty acids and their heterocyclic derivatives. *Eur J Pharmacol*. 2020;871. doi:10.1016/J.EJPHAR.2020.172937
68. Pacheco BS, Dos Santos MAZ, Schultze E, et al. Cytotoxic activity of fatty acids from Antarctic macroalgae on the growth of human breast cancer cells. *Front Bioeng Biotechnol*. 2018;6:185. doi:10.3389/FBIOE.2018.00185/BIBTEX
69. Slim R, Hammock BD, Toborek M, et al. The role of methyl-linoleic acid epoxide and diol metabolites in the amplified toxicity of linoleic acid and polychlorinated biphenyls to vascular endothelial cells. *Toxicol Appl Pharmacol*. 2001;171(3):184–193. doi:10.1006/TAAP.2001.9131
70. Casillas-Vargas G, Ocasio-Malavé C, Medina S, et al. Antibacterial fatty acids: an update of possible mechanisms of action and implications in the development of the next-generation of antibacterial agents. *Prog Lipid Res*. 2021;82:101093. doi:10.1016/J.PLIPRES.2021.101093